# ASYMMETRIC BISTABILITY IN THE RÖSSLER SYSTEM*

Julien Clinton Sprott

Department of Physics, University of Wisconsin–Madison
Madison, WI 53706, USA

Chunbiao Li[†]

Jiangsu Key Laboratory of Meteorological Observation
and Information Processing
Nanjing University of Information Science & Technology
Nanjing 210044, China
and
School of Electronic & Information Engineering
Nanjing University of Information Science & Technology
Nanjing 210044, China

Symmetric pairs of coexisting attractors are commonly found in symmetric dynamical systems when symmetry breaking occurs. By contrast, asymmetric bistability is rarely reported in either symmetric or asymmetric dynamical systems because such behavior typically occurs in narrow regions of parameter space and thus is often unnoticed. This paper describes an exploration of the regular parameter space of the Rössler system and shows examples of strange attractors coexisting with other strange attractors and with limit cycles, and asymmetric pairs of limit cycles in limited parameter space. A particular 1D path through parameter space is chosen to illustrate the various regions and the bifurcations that accompany the birth and death of the coexisting asymmetric attractors.

---

† Corresponding author: `goontry@126.com`; `chunbiaolee@nuist.edu.cn`

## 1. Introduction

In 1976 and 1979, Rössler proposed a class of relatively simple chaotic system [1, 2]. Like the Lorenz system [3], it has three variables, seven terms, and three parameters, but only a single quadratic nonlinearity. Because of its simplicity, the Rössler system has been widely used for studying chaos and related theoretical and experimental topics [4–17] such as bifurcations and evolutions [4–8], optimal control [10, 11], optimal synchronization [12, 13], and some topics associated with multistability [14–17]. Hens *et al.* [14] predicted extreme multistability in a system of two coupled Rössler oscillators, and later Patel *et al.* [15] provided experimental observations of that multistability in an electronic system consisting of two coupled Rössler oscillators. Postnov *et al.* [16] gave numerical examples using coupled Rössler systems and model maps to explain the role of multistability in the transition to chaotic phase synchronization. Chandrasekar *et al.* [17] confirmed the ubiquitous nature of the intensity induced chimeras by a system of globally coupled Rössler oscillators. However, multistability in a single Rössler system has been relatively little studied [4, 18].

Multistability is important because it is a common phenomenon in nature and can lead to unexpected and disastrous consequences in practical engineering applications. Consequently, it has been of considerable interest to scientists and has led to much active research [18–28]. Symmetric dynamical systems are prone to produce a symmetric pair of coexisting attractors [18, 23–26] when the symmetry of the solution is broken. However, asymmetric systems can also exhibit multistability [27, 28]. Sprott *et al.* [27] showed that even a simple three dimensional system can have three different kinds of coexisting attractors, including point, periodic, and strange attractors. Line equilibria in a system [28] can give different stability in the neighborhood of the line, which also leads to different asymmetric multistable states. Since the Rössler system has a simple asymmetric structure that gives chaos, it is natural to ask if it has a normal region where coexisting asymmetric attractors occur besides the cases mentioned by Barrio *et al.* [4].

Although multistability poses threats in some practical applications, asymmetric multistability, especially coexisting attractors with different manifolds, has potential value in other applications. For example, in electronic engineering, versatile analog signal generators can exploit changes in initial conditions to alter the type of oscillation, which is easier to produce with programmable technology than selecting different circuit parameters. In addition, multistability is a common property of neural networks that permit certain applications where monostable systems could be computationally restrictive [29]. Multistability of cellular neural networks can also be applied to increase the storage capacity of associative memories [29, 30].

   Motivated by the wide focus on the Rössler system and the interest in multistability, we explored the 3D parameter space for new examples of multistability in the Rössler system. Barrio *et al.* [4] have given a qualitative analysis of the Rössler equation and mentioned several regimes of bistability. However, their system parameter $c$ is very large (like $c = 48.5$) and all variables oscillate violently with large amplitude in contrast to the behavior of the conventional Rössler system. Here, we report bistability in the normal range of parameters and show the various regimes of bistability and the bifurcations that accompany the birth and death of the coexisting asymmetric attractors. Freire *et al.* [5] studied the triple-zero bifurcation in the 1979 Rössler equation, which is equivalent to the 1976 Rössler system in the region where the equilibria exist. However, the chaotic attractors in the 1979 Rössler system near the triple-zero degeneracy were spiral chaotic attractors or screw chaotic ones. Our study of bistability shows that those coexisting strange attractors in the 1976 Rössler system are basically spiral chaotic attractors. In Section 2, we report coexisting strange attractors in the Rössler system. In Section 3, the bifurcations are analyzed along a particular 1D path through parameter space, and additional examples of multistability are found. Conclusions are given in the last section.

## 2. Asymmetric strange attractors

   The familiar Rössler system [1] is given by:

$$\begin{aligned}
\dot{x} &= -y - z\,, \\
\dot{y} &= x + ay\,, \\
\dot{z} &= b + z(x - c)\,.
\end{aligned} \tag{1}$$

When $a = b = 0.2$, $c = 5.7$, the system is chaotic, as shown in Fig. 1 with Lyapunov exponents (LEs) of $(0.0714, 0, -5.3943)$ and a Kaplan–Yorke dimension of $D_{\mathrm{KY}} \approx 2.0132$. The largest LE is calculated numerically by following a reference trajectory and a nearby satellite trajectory whose distance but not direction is readjusted at every time step. The largest LE $(\lambda_1)$ is determined from the average of the logarithm (base $e$) of the growth in distance for each time step divided by the size of the time step. The other two LEs are determined using the fact that one must be zero and the sum of the three is the average rate of state space expansion, which is determined from the time average of the trace of the Jacobian matrix [31, 32]. From the LE spectrum, the Kaplan–Yorke dimension is determined from $D_{\mathrm{KY}} = 2 - \lambda_3/\lambda_1$ whose value for the standard Rössler system (1) is close to 2.0296 [32].
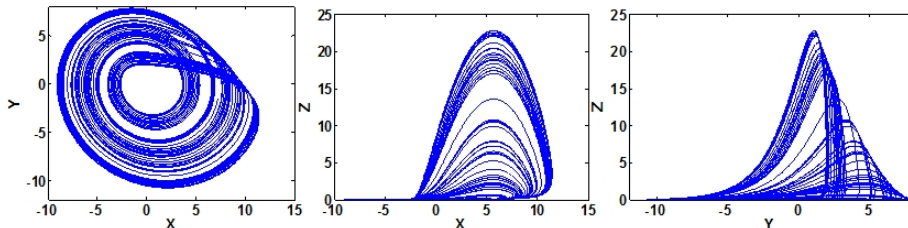
Fig. 1. (Color online) Rössler attractor from system (1) with $a = b = 0.2$, $c = 5.7$ and initial conditions $(x_0, y_0, z_0) = (-9, 0, 0)$.

Modern computers are capable of examining millions of parameter combinations and initial conditions, seeking cases for which different initial conditions produce different attractors for the same parameter values. The algorithm used for finding coexisting attractors is as follows:

(I) Chose the parameters $(a, b, c)$ randomly from a Gaussian distribution with unit variance centered on the origin, but allow the center of the Gaussian to wander around the parameter space by moving it to the location of where a new bistable solution is found.

(II) For each parameter combination, two initial conditions are chosen randomly from a Gaussian distribution of unit variance centered on the last bistable case that was found, and a quantity that is expected to be different such as the center of mass is calculated for each attractor.

(III) Since the position of the center of mass of different attractors may be similar, a more complicated quantity given by the time average of $x + |x| + y + |y| + z + |z|$ was used, and the criterion for bistability was taken as a 10% difference in this value for the two chosen initial conditions. No effort was made to find cases with more than two coexisting attractors. The vast majority of the cases fail this test, but out of millions of trials, dozens of bistable candidates were identified.

This algorithm found a number of cases where there are two coexisting strange attractors in the Rössler system, one example of which occurs for $a = 0.29$, $b = 0.14$, $c = 4.52$ shown in Fig. 2 with the waveform shown in Fig. 3. These two attractors have different Lyapunov exponents (LEs) of $(0.0397, 0, -3.6120)$ and $(0.0346, 0, -3.8953)$, respectively, and the corresponding Kaplan–Yorke dimensions $D_{KY}$ are 2.0110 and 2.0089. These two coexisting strange attractors are different in shape and size, in contrast to the symmetric pairs that are frequently found in symmetric systems with symmetry breaking. Additionally, their basins of attraction are not a symmetric pair. Figure 4 shows a cross section of the highly structured basins of attraction of the asymmetric strange attractors in the plane $z = 15.55517$, where one of the two equilibrium points lies. In the white region exterior to the basins, orbits are unbounded.
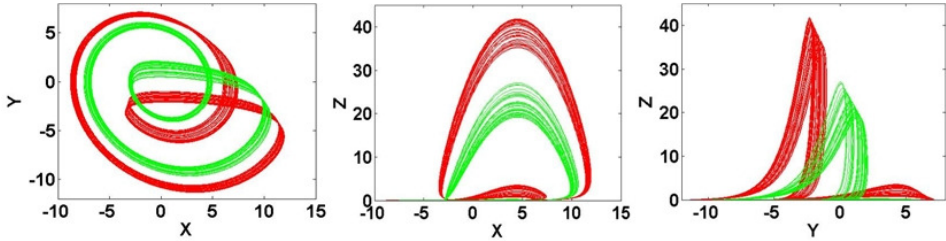
Fig. 2. (Color online) Asymmetric strange attractors in the Rössler system (1) for $a = 0.29$, $b = 0.14$, $c = 4.52$; black/red and gray/green attractors correspond to the initial conditions IC1 $= (-1.25, -0.72, -0.10)$ and IC2 $= (0.72, 1.28, 0.21)$, respectively.
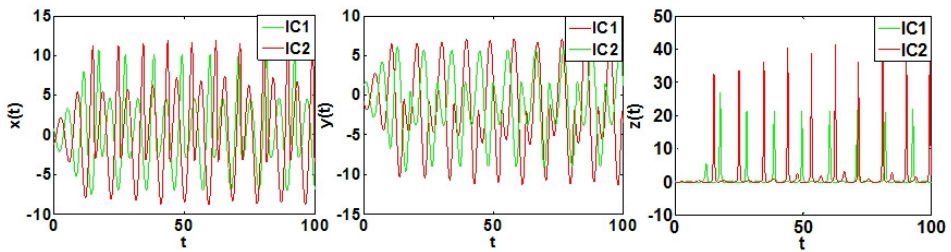


Fig. 3. (Color online) Waveforms of the two coexisting strange attractors in the Rössler system (1) for $a = 0.29$, $b = 0.14$, $c = 4.52$ — black/red for IC1 and gray/green for IC2.
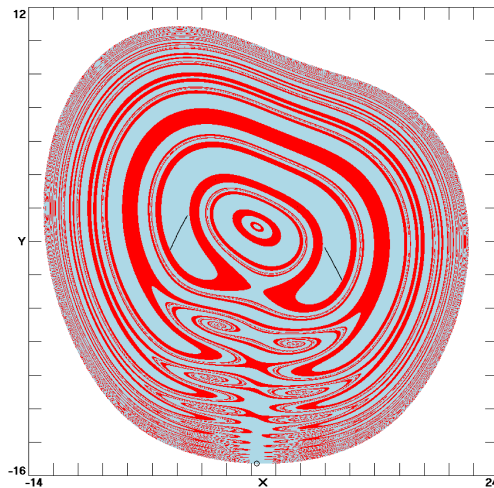


Fig. 4. (Color online) Cross section for $z = 15.55517$ of the basins of attraction (gray/light blue and black/red) for the coexisting asymmetric strange attractors at $a = 0.29$, $b = 0.14$, $c = 4.52$.

The two equilibrium points $E_{1,2} = (\frac{c \mp \sqrt{Q}}{2}, \frac{-c \pm \sqrt{Q}}{2a}, \frac{c \mp \sqrt{Q}}{2a})$ exist when $Q = c^2 - 4ab \geq 0$. The one at $E_1$ is close to the origin, while $E_2$ is more remote. Specifically, when $a = 0.29, b = 0.14, c = 4.52$, the two equilibrium points are $E_1 = (0.0090, -0.0310, 0.0310)$ and $E_2 \approx (4.5110, -15.5552, 15.5552)$, which are a saddle focus with index-2 indicated by one real negative eigenvalue, and a complex conjugate pair with a positive real part, and a spiral repellor with index-3 indicated by one real positive eigenvalue, and a complex conjugate pair with a positive real part, respectively, according to their eigenvalues $(0.1417 \pm 0.9896i, -4.5044)$ and $(0.2720, 0.0045 \pm 4.0682i)$. Contrast these values with those for the standard Rössler system with parameters $a = b = 0.2, c = 5.7$, where the two equilibrium points are spiral saddles at $(0.0070, -0.0351, 0.0351)$ and $(5.6930, -28.4649, 28.4649)$ with eigenvalues $(0.0970 \pm 0.9952i, -5.6870)$ and $(0.1930, -0.0000 \pm 5.4280i)$, indicating they are index-2 and index-1, respectively.

The equilibrium point $E_1$ lies on the basin boundary between the two strange attractors, presumably with its unstable manifold tangent to the boundary. Initial conditions in the immediate vicinity of the equilibrium are about equally likely to end up on either attractor. Thus, the attractors are self-excited but could easily be missed if only one initial condition near the equilibrium were chosen. The other equilibrium point $E_2$, shown as a small circle at the bottom center of Fig. 4, lies on the basin boundary of one of the strange attractors, with some initial conditions in its vicinity going to the attractor with others going to infinity. The basins have the expected asymmetry about the $z$-axis and a fractal structure. The black lines are cross sections of the corresponding strange attractors that nearly touch their basin boundaries. Therefore, neither of these attractors is hidden [33–36], but there could be others that are.

## 3. Bifurcations analysis

To explore the bifurcations and look for additional examples of bistability, we define a new parameter $\alpha$ and construct a one-dimensional straight-line path through the three-dimensional parameter space that passes though the values for the standard Rössler attractor $(0.2, 0.2, 5.7)$ when $\alpha = 0$ and through the parameters where two strange attractors coexist $(0.29, 0.14, 4.52)$ when $\alpha = 1$,

$$\begin{cases} a = 0.2 + 0.09\alpha, \\ b = 0.2 - 0.06\alpha, \\ c = 5.7 - 1.18\alpha. \end{cases} \tag{2}$$

Along this path, limit cycles and strange attractors occur over the range $[-2.2, 1.8]$, and the corresponding bifurcations are shown in Fig. 5. The

equations are solved using a fourth order Runge–Kutta integrator with adaptive step size with a largest value of 0.005. In this figure, $\alpha$ is slowly increased from $-2.2$ with the quantities plotted in red and then slowly decreased from $\alpha = 1.8$ with the quantities plotted in green without changing the initial conditions during the evolvement of the parameter. Regions where the two curves overlap are plotted in black. Thus, areas of hysteresis and bistability are indicated by the coexistence of solid red and solid green. In the figure, $A$ is the square root of the time average of $(x-1.6)^2 + (y-1.6)^2 + (z-1.6)^2$, which is an arbitrary quantity intended unlikely to be the same for two coexisting attractors and is plotted for the reference initial condition and for one chosen randomly from its Gaussian neighborhood, $L$ is the largest Lyapunov exponent, $K$ is the Kaplan–Yorke dimension, and $M$ is the local maximum values of the variable $x$. The quantity $A$ is multivalued wherever there are coexisting attractors, even ones not resulting from hysteresis.
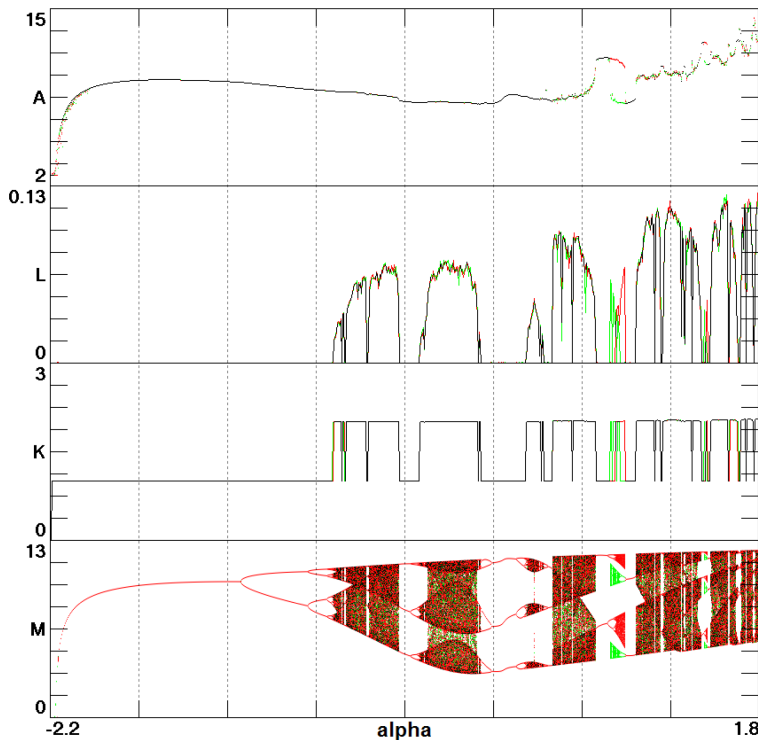


Fig. 5. (Color online) Bifurcation diagram when $\alpha$ varies in the region $[-2.2, 1.8]$.

For $\alpha < -2.17$, the equilibrium near the origin is stable and attracts initial conditions within its large basin of attraction. When $\alpha$ varies in the selected region, a supercritical Hopf bifurcation of the equilibrium $E_2$

occurs at $\alpha \approx -2.17$ giving birth to a limit cycle with an angular frequency $\omega = 1.0$, which can be verified algebraically according to the Andronov–Hopf bifurcation theorem with the characteristic equation $F(\lambda) = \lambda^3 + (c - a - x)\lambda^2 + (ax - ac + z + 1)\lambda - az - x + c = 0$. Some other bifurcations along different parameter paths are shown in [4]. After that, there is a typical period-doubling sequence of bifurcations until chaos onsets at $\alpha \approx -0.60$. The interval $\alpha \in (-0.6, 1.8)$ is chaotic with numerous periodic windows including the region around $\alpha = 1.0$ where the two strange attractors coexist as shown in Fig. 2. The strange attractor is destroyed around $\alpha = 1.85$, presumably in a boundary crisis.

The largest region of bistability occurs around $\alpha \in (0.95, 1.05)$ as shown in more detail in Fig. 6. This structure repeats on ever smaller scales in the (presumably infinitely many) periodic windows in the range of $\alpha \in (1.2, 1.8)$. The coexisting strange attractors within the periodic windows have their own periodic windows, which implies that there are places such as $\alpha = 1.03$ where a limit cycle coexists with a strange attractor as shown in Fig. 7. These limit cycles undergo a period doubling route to chaos, which means
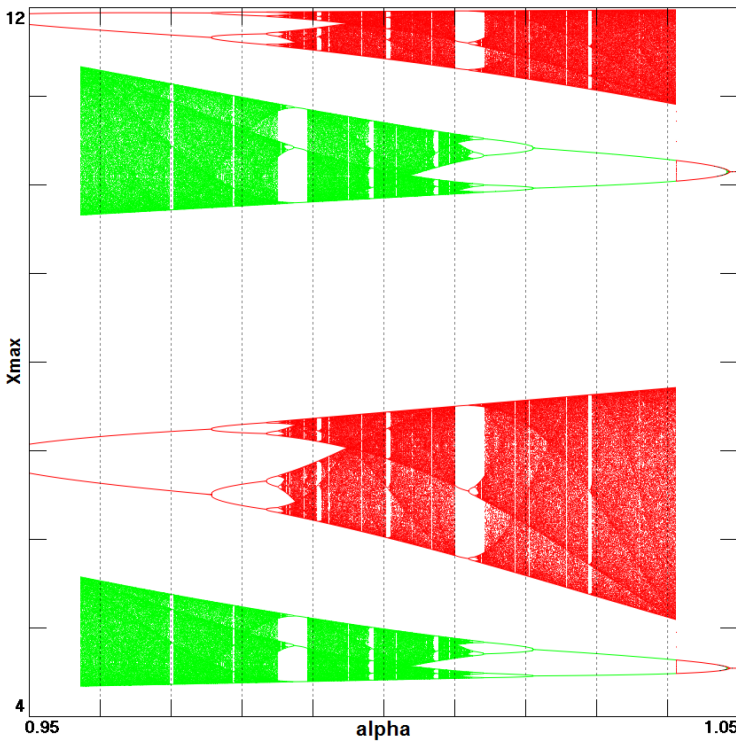


Fig. 6. (Color online) Bifurcation diagram in the region of coexistence $[0.95, 1.05]$ with an upward sweep (black/red) and a downward sweep (gray/green).

that the strange attractor can coexist with limit cycles of arbitrarily large periods. However, the periodic windows of these coexisting attractors stubbornly refuse to overlap anywhere along this path through parameter space, although there are other parameters such as $\alpha = 0.595$, where asymmetric limit cycles coexist as shown in Fig. 8. These coexisting limit cycles appear not to result from hysteresis.
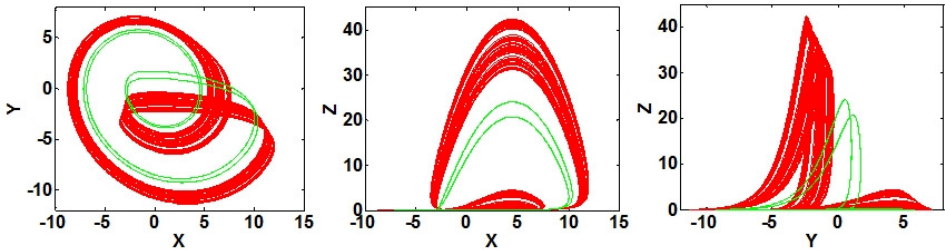


Fig. 7. (Color online) Coexisting strange attractor and limit cycle in the Rössler system for $\alpha = 1.03$ ($a = 0.2927, b = 0.1382, c = 4.4846$). Black/red and gray/green attractors correspond to two different initial conditions $(-2, 1.28, 0.21)$ and $(1.5, 1.28, 0.21)$.
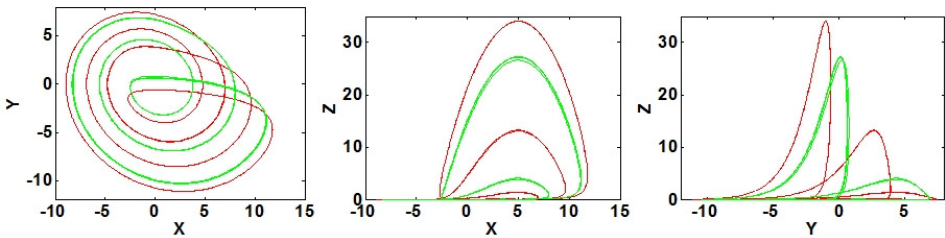


Fig. 8. (Color online) Coexisting limit cycles in the Rössler system for $\alpha = 0.595$ ($a = 0.2536, b = 0.1643, c = 4.9979$). Black/red and gray/green attractors correspond to two different initial conditions $(0, 7.2, 0.3)$ and $(3, 2.31, 0.1)$.

A similar computer search was unsuccessful for finding chaotic or periodic solutions in the absence of any equilibria when $Q = c^2 - 4ab < 0$ or when the one close to the origin is stable according to the Routh criterion. So in the whole parameter space, the Rössler system probably has no hidden attractors, and no other types of bistability were found.

## 4. Conclusions

Despite its considerable interest and widespread use, the Rössler system has previously unexplored regions in parameter space where it is bistable with coexisting strange attractors and limit cycles. One particular path through parameter space has been explored in detail here. It seems likely that there are yet other regions in the three-dimensional parameter space, including negative values of the parameters, where additional bifurcations and examples of multistability exist. We encourage others to continue examining this venerable and dynamically rich system.

## REFERENCES

[1] O.E. Rössler, *Phys. Lett. A* **57**, 397 (1976).

[2] O.E. Rössler, *Ann. NY Acad. Sci.* **316**, 376 (1979).

[3] E.N. Lorenz, *J. Atmos. Sci.* **20**, 130 (1963).

[4] R. Barrio, F. Blesa, S. Serrano, *Physica D* **238**, 1087 (2009).

[5] E. Freire, E. Gamero, A.J. Rodriguez-Luis, A. Algaba, *Int. J. Bifurcat. Chaos* **12**, 2799 (2002).

[6] A. Algaba, E. Freire, E. Gamero, A.J. Rodriguez-Luis, *Phys. Lett. A* **379**, 1114 (2015).

[7] D.H. Zanette, A.S. Mikhailov, *Phys. Rev. E* **62**, R7571 (2000).

[8] J.F. Chang *et al.*, *Chaos Soliton Fract.* **37**, 609 (2008).

[9] I.A. Garcia, J. Llibre, S. Maza, *Phys. Lett. A* **376**, 2234 (2012).

[10] M. Rafikov, J.M. Balthazar, *Phys. Lett. A* **333**, 241 (2004).

[11] H. Zhang, X. Ma, M. Li, J. Zou, *Chaos Soliton Fract.* **26**, 353 (2005).

[12] A. Ei-Gohary, *Chaos Soliton Fract.* **27**, 345 (2006).

[13] Z. Yan, *Phys. Lett. A* **334**, 406 (2005).

[14] C. Hens, R. Banerjee, U. Feudel, S.K. Dana, *Phys. Rev. E* **85**, 035202(R) (2012).

[15] M.S. Patel *et al.*, *Phys. Rev. E* **89**, 022918 (2014).

[16] D.E. Postnov *et al.*, *Chaos* **9**, 227 (1999).

[17] V.K. Chandrasekar, R. Gopal, A. Venkatesan, M. Lakshmanan, *Phys. Rev. E* **90**, 062913 (2014).

[18] C. Li, W. Hu, J.C. Sprott, X. Wang, *Eur. Phys. J. Special Topics* **224**, 1493 (2015).

[19] V.N. Chizhevsky, *J. Opt. B: Quantum Semiclass. Opt.* **2**, 711 (2000).

[20] P.R. Sharma, M.D. Shrimali, A. Prasad, U. Feudel, *Phys. Lett. A* **377**, 2329 (2013).

[21] E.L. Rempel, A.C.-L. Chian, *Phys. Rev. E* **71**, 016203 (2005).

[22] S. Banerjee, *IEEE Trans. Circ. Syst.-I: Fundam. Theory Appl.* **44**, 847 (1997).

[23] C. Li, J.C. Sprott, *Int. J. Bifur. Chaos* **23**, 1350199 (2013).

[24] C. Li, J.C. Sprott, *Phys. Lett. A* **378**, 178 (2014).

[25] C. Li, J.C. Sprott, *Int. J. Bifur. Chaos* **24**, 1450131 (2014).

[26] C. Li, J.C. Sprott, *Int. J. Bifur. Chaos* **24**, 1450034 (2014).

[27] J.C. Sprott, X. Wang, G. Chen, *Int. J. Bifur. Chaos* **23**, 1350093 (2013).

[28] S. Jafari, J.C. Sprott, *Chaos Solitons Fractals* **57**, 79 (2013).

[29] Z. Zeng, T. Huang, W. Zheng, *IEEE Trans. Neural Network* **21**, 1371 (2010).

[30] Z. Zeng, W. Zheng, *IEEE Trans. Neural Networks Learn. Syst.* **23**, 293 (2000).

[31] N.V. Kuznetsov, T.A. Alexeeva, G.A. Leonov, *Nonlinear Dynam.* **85**, 195 (2016) [arXiv:1410.2016 [nlin.CD]].

[32] N.V. Kuznetsov, T.N. Mokaev, P.A. Vasilev, *Commun. Nonlinear Sci. Numer. Simulat.* **19**, 1027 (2014).

[33] G.A. Leonov, N.V. Kuznetsov, *Int. J. Bifur. Chaos* **23**, 1330002 (2013).

[34] G.A. Leonov, V.I. Vagaitsev, N.V. Kuznetsov, *Eur. Phys. J. Special Topics* **224**, 1405 (2015).

[35] G.A. Leonov, V.I. Vagaitsev, N.V. Kuznetsov, *Phys. Lett. A* **375**, 2230 (2011).

[36] G.A. Leonov, V.I. Vagaitsev, N.V. Kuznetsov, *Physica D* **241**, 1482 (2012).